Wragge-Morley, R. T., Herrmann, G., Burgess, S., & Barber, P. (2016). Modelling and Simulation of Rapidly Changing Road Gradients. SAE International Journal of Passenger Cars - Mechanical Systems, 9(1), 392-401. DOI: 10.4271/2016-01-1663

2016-01-1663

Modelling and Simulation of Rapidly Changing Road Gradients

Author, co-author (Do NOT enter this information. It will be pulled from participant tab in MyTechZone)

Affiliation (Do NOT enter this information. It will be pulled from participant tab in MyTechZone)

Abstract

In vehicle dynamics modelling, the road profile is generally treated in one of two ways; either the gradient is a property that changes over a length scale far greater than that of the vehicle's wheelbase, or as a very detailed road surface model for determining the behaviour of vehicle suspensions. Occasionally, for modelling the behaviour of off-road vehicles, step-climbing manoeuvres are modelled. We propose an extension of these step-climbing models to a general, continuously varying road gradient model for cases where the distance over which the large gradient change occurs are of similar length-scale as the vehicle wheelbase. The motivation behind this work comes from a road gradient and vehicle mass estimation problem where it was noticed that very sudden gradient changes have a significant impact on the powertrain, but in a way that is not proportional to the attitude change of the vehicle. We present an analysis applicable to these cases where the road gradient change is substantially different from the vehicle attitude change. The analysis is built up from a very basic step climbing exercise to a general case solution for two dimensional longitudinal vehicle dynamics. Methods of handling road gradient and gradient change for modelling purposes are discussed. A method is proposed that defines the gradient change as an input to a backwards dynamic model that allows us to compute torque required to achieve a pre-defined datum speed during a gradient transition. The results of simulations for simple gradient change cases are shown. We discuss the implication of these road gradient transients for vehicle parameter estimation based on powertrain behaviour.

1. Introduction

The vast majority of gradient estimation work focuses on macro-scale changes of gradient, such as those found on highways. In this case, it is certainly the case that the road gradient is, as most established literature [1] [2] [3] [4] [5] asserts, a property that affects the whole vehicle equally, and so can be treated as an individual parameter at any point in time. However, there is a family of specific cases, perhaps more relevant to off-road driving, where the road gradient changes very suddenly; for the sake of argument, we shall suppose this to mean the road gradient changing appreciably within the wheelbase length of the vehicle. Since road gradient estimation is often carried out using driveline torque as an input [6] [7] [8] it is important to consider the relationship between driveline torque and road gradient. In this paper we present an analysis of the kinematics and dynamics of a rapidly changing gradient scenario, which should be of interest to vehicle dynamics and control engineers seeking to understand the fluctuations in powertrain load and expected accelerations in such a situation and develop solutions with these dynamics in mind.

Substantial work has been carried out into the estimation of macro-scale road gradient as a vehicle parameter. This is often undertaken in conjunction with the estimation of vehicle mass, since the two are coupled through the vehicle dynamics by Newton's Second Law. The authors of this paper have devoted a substantial research effort to estimation problems of this type [6] [7] [9] [10] using a novel adaptive filtering system as an estimation algorithm. The interest in this research is driven by the increase in levels of functionality and autonomy in vehicle embedded systems and the requirement for accurate vehicle system models.

Numerous approaches to estimation problems of this type also exist in the literature, including work by Sahlholm et al. [11] [12] [13] considering the learning of road gradient profile over multiple passes along the same route by heavy duty vehicles. Recursive Least Squares methods are common for estimation of multiple parameters, for instance, Vahidi [14] estimates road gradient and mass simultaneously. Many approaches use a combination of RLS and Kalman Filtering methods to simultaneously estimate road gradient and vehicle mass, including Raffone [8] and Vahidi [14]. Nonlinear observer structures are also used, by the current authors [9] [10] [15] [7] and by McIntyre [16] and Rajamani [17].

The other extreme of length scale for road gradient is estimation of surface roughness imperfections, which are either generally examined as a frequency domain problem for suspension and design for Noise Vibration and Harshness (NVH) [2] [18], or sometimes as an estimation problem in their own right. The problem of developing a 'profilometer' was initially tackled in the 1960s by Spangler et al. [19] at General Motors Research in order to develop models for the analysis of suspension performance, whilst Sayers et al [20] developed a 'longitudinal profile analyser' at LCPC[1] as part of the International Road Roughness Experiment. More recently, Imine et al [21] used both the 'lpc' method and a sliding mode observer method to estimate road profile with some success; Doumiati. et al [22] have employed Kalman Filtering [23].

In the case where the gradient change in the vehicle length scale is minimal, the resistive load due to gravity experienced by the drivetrain is a function of that road gradient. However, in the case

[1] Laboratoire central des ponts et chaussées

where the road gradient changes substantially within the wheelbase length of the vehicle, it is clear that the work done against gravity must still be proportional to the rate of height gained by the centre of mass. In the changing gradient case, this is now dependent on the gradient of the road at the two contact points and the instantaneous inclination of the vehicle, as well as the rate of change of inclination. Naturally, the more realistic vehicle dynamics are included in such a problem, the more complex it gets.

A similar case often presented in the literature [24] considers a vehicle which climbs a small step. This is a common problem for off-road vehicle dynamics and may be used in design of powertrain and tyre sizing; of course this problem may be examined at differing levels of complexity, and is frequently limited to fairly simple tyre models to ease analysis. The work presented in this paper is concerned with what may be considered an extension of the 'step climbing' problem. Several illustrative cases are presented in section 2 that examine the behaviour of a vehicle with its front and rear contact patches on roads of different gradients. These cases are used to develop a set of geometrical relations for a general problem containing two road gradients. Implementation of the kinematics in stepwise, discrete time simulation is presented in section 3 and a backwards model of the vehicle dynamics, where driving force is calculated from the kinematic relationships based on a defined speed, is presented in section 4. Several different approaches to handling the problem in simulation are discussed and results are presented in section 5.

2. An Illustration of the changing gradient problem.

In order to demonstrate how the locus of the position of the centre of mass of a two-axled, rigid vehicle varies whilst undergoing a gradient transition, we shall provide a series of examples beginning with a simple, albeit unrealistic, right angle step climbing exercise. Initially we shall consider the geometric relationships and then build up a general model of the dynamics of the gradient change scenario.

Right Angle Step

This example is essentially the same as the classic 'ladder sliding down a wall' problem. Each contact point is resting on a smooth flat plane. The angle of the plane on which the front contact point rests is θ_f and the plane on which the rear rests is at an angle θ_r. The two planes meet at a sharp join. The vehicle body is represented by a rigid bar of length L_c instantaneously inclined at an angle θ_c from the horizontal and of mass m. The centre of mass, for purposes of simplification shall be considered to be at some length along this bar, L_f from the front contact point and L_r from the rear contact point. In the analysis of the following examples, we shall consider the kinematics from the instant that the front contact point begins its new trajectory so that the distance from the rear contact point to the junction of the two planes at time $t = 0$ is equal to the wheelbase length L_c and the displacement of the front and rear contact points on their respective trajectories is s_f and s_r.

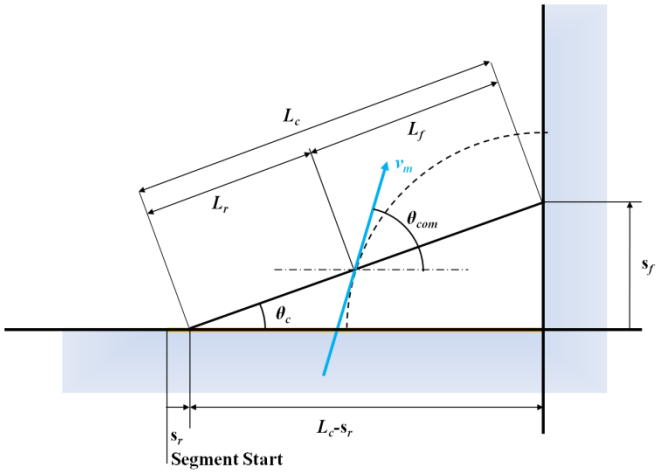

Figure 1. The simplest way of illustrating the changing gradient problem is by examining a simple step climbing example. The labelled angles in this illustration are the angle of inclination of the vehicle θ_c and the angle of the tangent to the centre of mass trajectory θ_{com}.

In this case, we may see that the relationship between front and rear displacement is, in the case of a right angle step, defined by Pythagoras' theorem.

$$L_c^2 = (L_c - s_r)^2 + s_f^2 \tag{1}$$

$$s_f = \sqrt{2L_c s_r - s_r^2} \tag{2}$$

The locus in this case is an eliptical path, or if the centre of mass is exactly halfway along the vehicle, a circular one. The gradient instantaneously experienced by the centre of mass is based on the relationship between the horizontal and vertical displacement of the rear and front axles respectively, which we have already derived. So the angle of inclination of the vehicle as a function of the displacements at a given instant is:

$$\theta_c = \tan^{-1}\left(\frac{s_f}{L_c - s_r}\right) \tag{3}$$

Since this case is a right angle, the path taken by the centre of mass may be split very neatly into its horizontal and vertical components:

$$\underline{\boldsymbol{s_{com}}} = [s_r + L_r(\cos\theta_c - 1)]\boldsymbol{i} + \left[\frac{L_r}{L_c}s_f\right]\boldsymbol{j} \tag{4}$$

where $s_f \equiv L_c \sin\theta_c$.

Thus it may be shown that the angle of the instantaneous gradient of the centre of mass in this case is,

$$\theta_{com} = \tan^{-1}\frac{ds_f}{ds_r} \tag{5}$$

General case for planar 'ramps'

This example concerns itself with the case where both the front and rear contact patches come to rest on ramps of non-zero gradient. We shall label the segments "f" and "r" for the front and rear contact respectively. A diagram explaining the nomenclature associated with

this case may be seen in Figure 2. Ignoring for the moment the actual transition from one ramp to the other, we can easily write relationships for the before and after transition cases where the two contact points move in parallel to one another, such that:

Table 1. Description of trajectories when both front and rear contact points are on the same plane.

Before	After
$\theta_{com} = \theta_{R_r}$	$\theta_{com} = \theta_{R_f}$
$\underline{\boldsymbol{s_{com}}} = s_r \cos\theta_{R_r}\boldsymbol{i} + s_r \sin\theta_{R_r}\boldsymbol{j}$ $\equiv s_f \cos\theta_{R_r}\boldsymbol{i} + s_f \sin\theta_{R_r}\boldsymbol{j}$	$\underline{\boldsymbol{s_{com}}} = s_r \cos\theta_{R_f}\boldsymbol{i} + s_r \sin\theta_{R_f}\boldsymbol{j}$ $\equiv s_f \cos\theta_{R_f}\boldsymbol{i} + s_f \sin\theta_{R_f}\boldsymbol{j}$

in these cases, $s_f = s_r = s_{com}$.

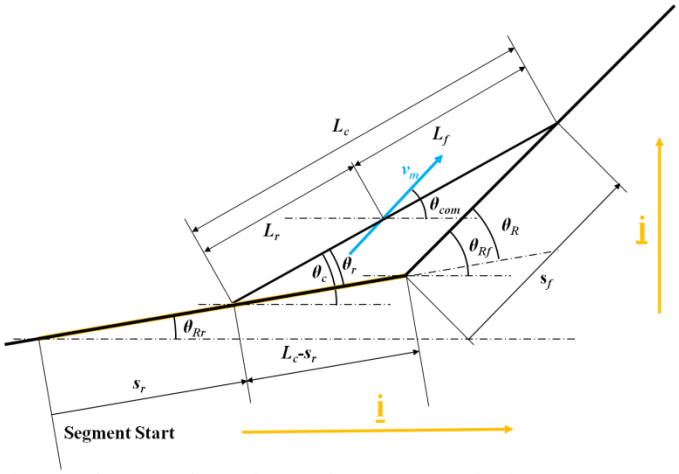

Figure 2. The 'General' case for two planar ramps meeting has non-zero road angle on each ramp, once again we consider the segment which starts at the point where the front wheel begins its new trajectory on the forward ramp. In this case, there are several additional angles to be considered and these are shown in the above diagram.

It is convenient for us to be able to write the angle of inclination of the vehicle body in terms of the road angles. Taking the triangle formed instantaneously by the wheelbase and the ramps, we may achieve this by rearranging the cosine rule as a quadratic equation (Equation (6)) giving a solution in the standard form (Equation (7)) with the terms described by Equations (8) – (10).

$$0 = b^2 - (2a\cos C)b + (a^2 - c^2) \quad (6)$$

$$b = \frac{-\beta \pm \sqrt{\beta^2 - 4\alpha\gamma}}{2\alpha} \quad (7)$$

$$\alpha = 1 \quad (8)$$

$$\beta = -2a\cos C \quad (9)$$

$$\gamma = a^2 - c^2 \quad (10)$$

where:

$$c \equiv L_c \quad (11)$$

$$a \equiv L_c - s_r \quad (12)$$

$$b \equiv s_f \quad (13)$$

$$C \equiv \pi - \theta_R = \pi - (\theta_{R_f} - \theta_{R_0}) \quad (14)$$

so that:

$$\alpha = 1 \quad (15)$$

$$\beta = -2(L_c - s_r)\cos(\pi - \theta_R) \quad (16)$$

$$\gamma = s_r^2 - 2L_c s_r \quad (17)$$

and:

$$s_f = (L_c - s_r)\cos(\pi - \theta_R) \pm \sqrt{(L_c^2 - 2L_c s_r + s_r^2)\cos^2(\pi - \theta_R) - s_r^2 + 2L_c s_r} \quad (18)$$

This allows us to write an expression for the inclination of the vehicle wheelbase in terms of the ramp angles; where $\theta_c(k)$ is calculated by applying the sine rule to the triangle formed by the road planes and the vehicle wheelbase, as illustrated in Figure 2. (n.b. the base of this triangle is already inclined at the angle (θ_{Rr}):

$$\theta_c = \theta_{R_r} + \sin^{-1}\left(\frac{s_f}{L_c}\sin(\theta_{R_f} - \theta_{R_r})\right) \quad (19)$$

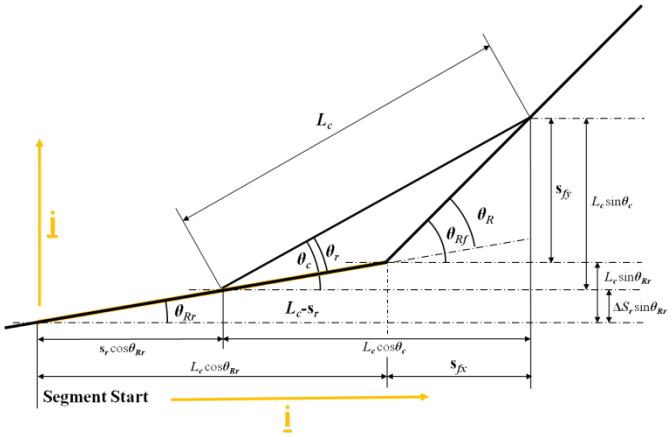

Figure 3. This case illustrates the **i and** j components in the horizontal and vertical directions of motion for the relative positions of the front and rear contact points.

For the purposes of illustrating this example, we shall take the rear wheel as the datum for displacement, just like in the vertical step example. As before we need to write down the geometric relationship between the displacement of the front and rear wheels. The horizontal and vertical components of displacement of both wheels are illustrated in Figure 3. From these relationships, we can write down the horizontal and vertical components of front contact point motion in terms of rear contact point displacement and current inclination of the vehicle body:

$$\underline{\boldsymbol{s_f}} = \left[s_r \cos\theta_{R_r} + L_c \cos\theta_c - L_c \cos\theta_{R_r}\right]\boldsymbol{i} + \left[s_r \sin\theta_{R_r} + L_c \sin\theta_c - L_c \sin\theta_{R_r}\right]\boldsymbol{j} \tag{20}$$

The vector displacement $\underline{\boldsymbol{s_f}}$ (or $\underline{\boldsymbol{s_r}}$ should we compute that) describes the scalar displacement s_f (or s_r etc.) used in equations (1) to (19) and elsewhere in the paper in terms of its x and y components.

Similarly, we may write the horizontal and vertical components of the centre of mass motion, s_{com}, which has its origin at the initial position of the centre of mass within the gradient change segment, in the following vector format.

$$\underline{\boldsymbol{s_{com}}} = \left[s_r \cos\theta_{R_r} + L_r \cos\theta_c - L_r \cos\theta_{R_r}\right]\boldsymbol{i} + \left[s_r \sin\theta_{R_r} + L_r \sin\theta_c - L_r \sin\theta_{R_r}\right]\boldsymbol{j} \tag{21}$$

This allows us to express the directions of the tangential velocity of the centre of mass as before.

$$\theta_{com} = \tan^{-1}\frac{\frac{d}{dt}\left[s_r \cos\theta_{R_r} + L_r \cos\theta_c - L_r \cos\theta_{R_r}\right]}{\frac{d}{dt}\left[s_r \sin\theta_{R_r} + L_r \sin\theta_c - L_r \sin\theta_{R_r}\right]} \tag{22}$$

In turn this allows us to write a derivative expression for the acceleration of the centre of mass in terms of the road angles and using one of the contact points as a datum for displacement.

$$\theta_{aoc} = \tan^{-1}\frac{\frac{d}{dt}\left[\frac{d}{dt}\left[s_r \cos\theta_{R_r} + L_r \cos\theta_c - L_r \cos\theta_{R_r}\right]\right]}{\frac{d}{dt}\left[\frac{d}{dt}\left[s_r \sin\theta_{R_r} + L_r \sin\theta_c - L_r \sin\theta_{R_r}\right]\right]} \tag{23}$$

3. Implementation of the kinematics calculation for simulation.

Here we present a formulation of the geometry that describes the motion of the centre of mass for the gradient change case between two planar ramps. We state certain necessary assumptions observed in this modelling exercise:

- The physical model of the road gradient in the x-z plane may be represented by a set of straight lines of a given length and angle.
- The instantaneous gradient of the contact patches at the front and rear is measured in the absolute sense from horizontal and may be different at the two axles. (When the vehicle wheelbase spans more than one sector of road).
- The model of the road must be handled in simulation as a set of segments, with segments starting and finishing each time one axle or another changes into a new sector.
- All measurement of displacement, including breakpoints between sectors are to be measured according to path length (ie. wheel displacement).
- For ease of illustration, the simulation development is treated in the discrete time, stepwise sense.
- That the time-step is much smaller than the time spent in each segment.

Let the initial condition of one axle be the zero datum point (in this case we shall select the front axle) and define the displacement along the two paths as scalar lengths s_f and s_r from the positions of the two contact points at this instant.

Using the discrete time step k and treating the change of displacement during the discrete step as $\Delta s(k)$; the displacement, in this case of the rear wheel, at a given time-step can be written in terms of the preceding one as

$$s_r(k) = s_r(k-1) + \Delta s_r(k) \tag{24}$$

where the change in displacement $\Delta s_r(k)$ during the discrete simulation step is defined as a function of its horizontal and vertical components:

$$\Delta s_r(k) = \sqrt{\Delta s_{xr}^2(k) + \Delta s_{yr}^2(k)} \tag{25}$$

The change of horizontal and vertical displacement is defined as

$$\Delta s_{xr}(k) = s_{xrS}(k) - s_{xrS}(k-1) \tag{26}$$

$$\Delta s_{yr}(k) = s_{yrS}(k) - s_{yrS}(k-1) \tag{27}$$

where the subscript S denotes displacement within the current gradient change segment. At this stage we can apply the trigonometry derived in section 2 to write:

$$s_{xrS}(k) = L_c \cos\theta_{Rr} + s_{fS}(k)\cos\theta_{Rf} - L_c \cos\theta_c(k) \tag{28}$$

$$s_{yrS}(k) = L_c \sin\theta_{Rr} + s_{fS}(k)\sin\theta_{Rf} - L_c \sin\theta_c(k) \tag{29}$$

where $\theta_c(k)$ is calculated by applying the sine rule to the triangle formed by the road planes and the vehicle wheelbase as in equation (19):

$$\theta_c(k) = \theta_{Rr} + \sin^{-1}\left(\frac{s_{fS}(k)\sin(\theta_{Rf} - \theta_{Rr})}{L_c}\right) \tag{30}$$

In our special case with planar ramps, and examining just one gradient transition, there is no change in road inclination with displacement within the segment, so the angles θ_{Rf} and θ_{Rr} may be considered to be known *a priori* in the context of this simulation method.

Implementing these equations allows us to generate the angles θ_{com} and θ_{aoc} according to the relationships described in equations (19) to (23).

4. Vehicle Dynamics: Implications of the centre of mass trajectory computation.

Work done to overcome road gradient, as experienced by the vehicle powertrain, is the work done to overcome the gain (or loss) in elevation with distance travelled. Therefore in the case of rapid gradient change, the value of the work done to overcome gravity is related to the trajectory of the centre of mass, rather than the inclination of the vehicle, which we have shown to be different properties. It is important to note, however, that certain other resistance forces are still dependent on either the angle of the road, in the case of tyre forces, or the attitude of the vehicle, for example aerodynamic drag. This complicates the summation of forces to compute the Newtonian force balance for the gradient changing case.

Dynamics at the centre of mass

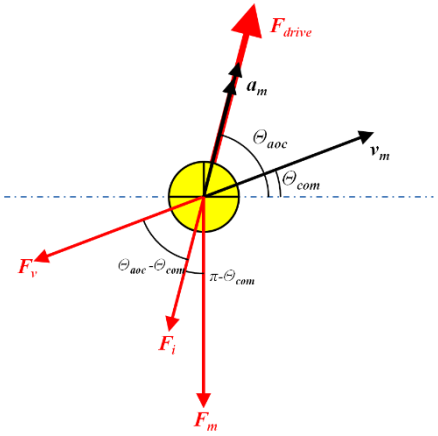

Figure 4. An illustration of an example set of forces acting on the centre of mass of the vehicle.

We shall first consider the centre of mass dynamics in isolation. An illustration of the directions these forces may act in is shown in Figure 4. The forces have been grouped into inertial forces that act in opposition to the direction of the acceleration of the centre of mass, velocity dependent forces that act in opposition to the tangential velocity of the centre of mass trajectory and gravitational forces. In this example it is assumed that the net driving force is in the direction of the acceleration of the centre of mass. This means that the centre of mass dynamics may be written as:

$$\ddot{s}_m = \frac{F_{drive}}{m} - g\cos\left(\frac{\pi}{2} - \theta_{aoc}\right) - \frac{F_v}{m}\cos(\theta_{aoc} - \theta_{com}) \tag{31}$$

where F_{drive} is the net driving force acting at the centre of mass, θ_{aoc} is the direction of acceleration of the centre of mass, and F_v is a resistive force term dependent on velocity; this term could encompass aerodynamics and viscous friction terms. The direction of the centre of mass velocity, θ_{com} is the angle instantaneously tangential to the trajectory of the centre of mass. In the diagram, $F_i = ma_m$ is the force due to translational inertia.

This of course is an over-simplification of the dynamics problem, since it does not take into account the individual contact patch forces or torques, nor the rotation of the vehicle body due to its change in attitude. In the next section we shall tackle a more complete version of this dynamics problem.

Inclusion of the contact patch forces in the vehicle dynamics

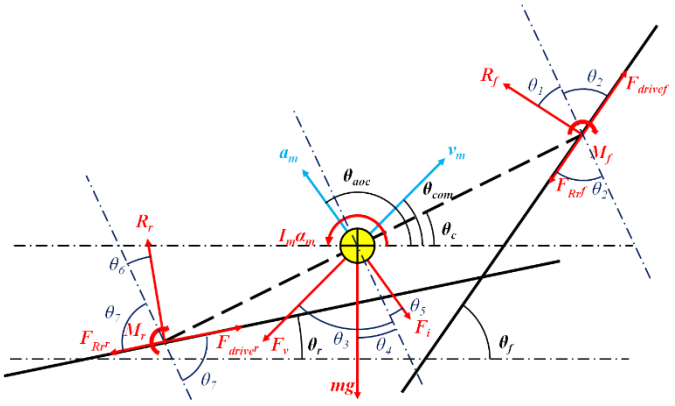

Figure 5. The complete set of torques and forces acting on the vehicle body during a period of gradient transition. For ease of notation, the critical angles have been numbered from θ_1 to θ_7. The definitions of these angles are presented in Table 2.

Table 2. Definition of the angles θ_1 to θ_7 as depicted in Figure 5. These angles are significant for the computation of the net forces acting on the centre of mass.

Angle	Defintion
$\theta_1 = \theta_{R_f} - \theta_c$	Angle between front normal force and the perpendicular to the
$\theta_2 = \theta_c - \theta_{R_f} + \frac{\pi}{2}$	Angle between front tangential forces and the perpendicular to the
$\theta_3 = \theta_c - \theta_{com} + \frac{\pi}{2}$	Angle between tangential velocity of the centre of mass and the perpendicular to the wheelbase
$\theta_4 = \theta_c$	Angle between gravitational force and the perpendicular to the
$\theta_5 = \theta_c - \theta_{aoc} + \frac{\pi}{2}$	Angle between centre of mass inertial force and the perpendicular to the wheelbase
$\theta_6 = \theta_c - \theta_{R_r}$	Angle between rear normal force and the perpendicular to the
$\theta_7 = \theta_{R_r} - \theta_c + \frac{\pi}{2}$	Angle between rear tangential forces and the perpendicular to the

In this section, we shall derive a backwards dynamic model to compute the variation in driving torques during a gradient change event of known kinematics.
The relationships in Table 2 allow us write down moment equations (Equations (35) to (37)) about the two contact points of the vehicle and thus compute the magnitudes of the normal reaction forces and required driving torque.

Forces acting perpendicular to the vehicle wheelbase

Using the angle definitions from Table 2, we may now define net forces acting perpendicular to the vehicle wheelbase at the front (Equation (32)), rear (Equation (33)) and centre of mass (Equation (34))

$$\sum F_f = R_f \cos\theta_1 + (F_{drive_f} - F_{RR_f})\cos\theta_2 \tag{32}$$

$$\sum F_r = R_r \cos\theta_6 - (F_{drive_r} - F_{RR_r}) \cos\theta_7 \quad (33)$$

$$\sum F_m = mg \cos\theta_4 + ma_m \cos\theta_5 \quad (34)$$

where $F_{drive_n} = {}^{M_n}/_{r_{eff_n}}$ is the driving is the driving force parallel to the road surface, $F_{RR_n} = C_\mu R_n$ is the rolling resistance, noting that $C_\mu$is dependent on other factors including wheelspeed. As defined elsewhere, m is the mass of the vehicle body, assumed to be concentrated at the centre of mass and g is the gravitational constant.

Following on from the definition of the grouped forces at each point along the vehicle wheelbase, we may now define moment and force balances to and determine expressions for the reaction and driving forces.

Moments about centre of mass

$$I_m\alpha_m = L_f \sum F_f - L_r \sum F_r + M_f + M_r \quad (35)$$

$$I_m\alpha_m = L_f R_f \cos\theta_1 + L_f (F_{drive_f} - F_{RR_f}) \sin\theta_1 - L_r R_r \cos\theta_6 - L_r (F_{drive_r} - F_{RR_r}) \sin\theta_6 + M_f + M_r \quad (36)$$

Noting once again that the rolling resistance force is a function of the normal reaction, $F_{RR_n} = C_\mu R_n$ and that, assuming no slip, the front and rear driving forces will for the sake of simplicity in our example be represented as functions of some powertrain torque M. In these expressions, $I_m\alpha_m$is the inertia due to the rotation of the vehicle body. The lengths L_f, L_r and L_c are the distance along the wheelbase that the various components act, defined in Figures 2 and 5. Thus our moment balance is in terms of the two normal reactions and driving torque, and is presented with the terms grouped in this manner in Equation (36):

$$I_m\alpha_m = [R_f \quad R_r \quad M] \begin{bmatrix} L_f(\cos\theta_1 - C_\mu \sin\theta_1) \\ L_r(-\cos\theta_6 - C_\mu \sin\theta_6) \\ \frac{1}{r}(L_f \sin\theta_1 + L_r \sin\theta_6) + 2 \end{bmatrix} \quad (37)$$

Cartesian components of force balance:

In a similar manner to solving a very involved version of the classic 'ladder sliding down a wall' dynamics problem, we now equate the horizontal and vertical components of the forces acting on the vehicle at a given instant and solve to give driving torque given an *a priori* defined set of kinematics. This allows us to illustrate the effect on the powertrain of passing through a sudden gradient transition.

Horizontal:

$$ma_m \cos\theta_{aoc} = -F_{RR_r} \cos\theta_{R_r} - R_r \sin\theta_{R_r} + F_{drive_r} \cos\theta_{R_r} - F_{RR_f} \cos\theta_{R_f} - R_f \sin\theta_{R_f} + F_{drive_f} \cos\theta_{R_f} \quad (38)$$

Vertical:

$$ma_m \sin\theta_{aoc} = -F_{RR_r} \sin\theta_{R_r} - R_r \cos\theta_{R_r} + F_{drive_r} \sin\theta_{R_r} - mg - F_{RR_f} \sin\theta_{R_f} - R_f \cos\theta_{R_f} + F_{drive_f} \sin\theta_{R_f} \quad (39)$$

These equations may now be re-written in the same manner as the moment equation to give a 'backwards' dynamic model in terms of the unknown reaction forces R_f and R_r and driving torque M. This model is presented with terms grouped in the same way as for the moment equations:

Horizontal:

$$ma_m \cos\theta_{aoc} = [R_f \quad R_r \quad M] \begin{bmatrix} -\sin\theta_{R_f} - C_\mu \cos\theta_{R_f} \\ -\sin\theta_{R_r} - C_\mu \cos\theta_{R_r} \\ \frac{1}{r}(\cos\theta_{R_f} + \cos\theta_{R_r}) \end{bmatrix} \quad (40)$$

Vertical:

$$ma_m \sin\theta_{aoc} = [R_f \quad R_r \quad M] \begin{bmatrix} \cos\theta_{R_f} - C_\mu \sin\theta_{R_f} \\ \cos\theta_{R_r} - C_\mu \sin\theta_{R_r} \\ \frac{1}{r}(\sin\theta_1 + \sin\theta_6) \end{bmatrix} - mg \quad (41)$$

where r is the rolling radius of the driving wheel in each case. The three expressions we have derived (Equations (37) and (40)-(41)) contain three unknowns and may be combined and solved simultaneously to give the normal reactions and driving torque for a given set of kinematics. The combined expression to be solved is given in Appendix A. Various dynamics, especially those concerning certain resistance losses, are unmodelled. In the majority of cases it would be straightforward to include forces such as air resistance as a function of velocity in the model we have developed. It is necessary to understand the direction and position on the vehicle where an additional force acts, or make appropriate assumptions to model these aspects of its behavior.

It should be noted at this point that in a real scenario, the torque distribution between front and rear wheels would typically be constrained, either passively or actively. This model, for illustrative purposes also assumes zero slip, an unlikely condition in the ascent of a very steep ramp in the real world. These and many other modelling considerations would need to be explored and developed in order to validate the model against a real extreme gradient change scenario.

5. Results

We present simulated results that illustrate the gradient change cases that we have developed in this paper. In order to present the kinematics and the backwards dynamic model we assume the speed at some datum (either the front or rear axle in our case) is controlled as an input to our analysis. In our example, we present an extreme case where a 1000kg vehicle transitions from a ramp of 0.1 radians to one of 1.5 radians. The wheelbase is set to be 3.5m and the reference speed is 1 ms^{-1} at the front axle. Thus the gradient transition begins at a datum displacement of 0m and ends at a displacement of 3.5m when the entire wheelbase is on the new gradient. In this example, zero slip is assumed, and we suppose that the vehicle is driven via

both contact patches, in this case both delivering a driving force equivalent to an identical torque M. Of course in reality this is an impossible scenario, but it serves to illustrate the idea presented in this paper.

In Figure 6. we examine the kinematic relationship between the front and rear wheels. The exaggeration of the difference in the relative displacement is dependent on the difference in angle between the centre of mass trajectory and the inclination of the vehicle. For the special case where the centre of mass is exactly half way between the front and rear wheels and the step being climbed is vertical, the trajectory followed by the centre of mass is perfectly circular assuming no compliance in the vehicle structure.

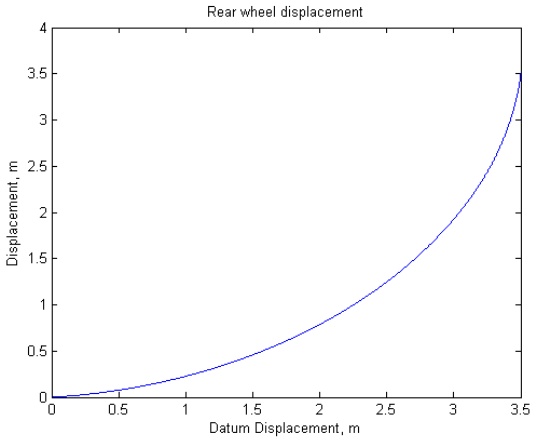

Figure 6. The relationship between front and rear wheel displacement for two ramps nearly at right angles to one another. The 'Datum Displacement' on the x-axis is the displacement of the front axle s_f, and the displacement s_r shown on the y-axis illustrates the nonlinearity between the front and rear motion due to the gradient transition.

The direction of the tangent to the vehicle mass is worth comparing to the angle of inclination of the vehicle body. Both are presented in Figure 7. This relationship illustrates quite clearly that it is inaccurate to assume the powertrain needs to overcome a gravitational force defined by $\boldsymbol{\theta_c}$ when the vehicle experiences a severe gradient change. Indeed, the reverse is true, insofar as upon meeting a sudden gradient change, the centre of mass initially begins to move on a trajectory with the same angle as the new gradient, whilst the inclination of the vehicle body remains almost parallel to the old one. As the vehicle body reaches the new gradient, the centre of mass is once again travelling almost parallel to the old gradient, with the consequence that the powertrain experiences less resistance due to gravity than one might expect at this attitude, before needing to propel the vehicle on the new trajectory, which once again requires a sudden increase in effort for very little change in attitude. This behaviour in the driving torque requirement to sustain a constant speed of the displacement datum in our example is presented in Figure 8.

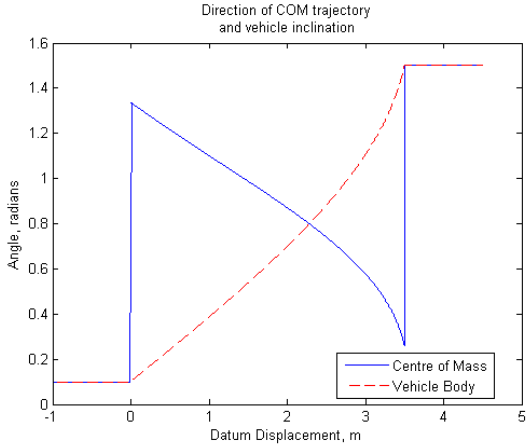

Figure 7. A comparison of the angles of the centre of mass trajectory θ_{com} and the inclination of the vehicle body θ_c during the gradient transition. Note the initial steepness of the centre of mass motion, and the second step in the gradient of the centre of mass trajectory once the rear axle reaches the second ramp.

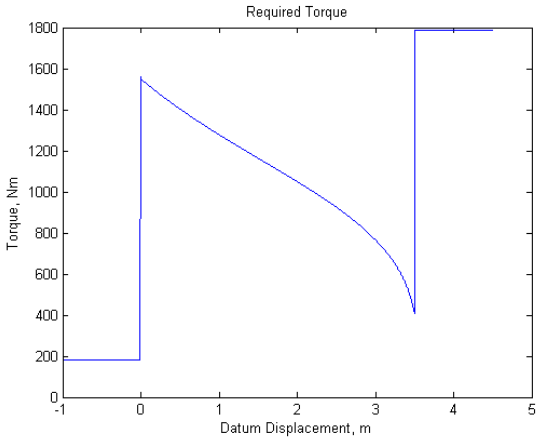

Figure 8. The change in driving torque M required at each wheel (assuming torques applied to each axle to be equal) during the gradient transition. The total torque required is double this value. Once again, note the 'two stage' behavior defining the start and end of the gradient transition.

6. Summary/Conclusions

In this paper we have discussed the behaviour of a vehicle undergoing a gradient transition and derived some simple example cases to illustrate the implications of these events for driveline torque dependent estimations. In many cases, either the rate or magnitude of transition render these effects negligible; but there is a substantial class of off-road driving events where these hitherto little examined dynamics combine with terramechanics and suspension dynamics to produce substantial disturbances to driveline torque.

From the perspective of the gradient and mass estimation problem that inspired this investigation, we should note that significant understanding has been gained. Examination of the results shows that on encountering a rapid change in path gradient, the torque demand to continue forwards motion will spike, then drop off as the centre of mass trajectory becomes parallel with the original path, then increase as a step when the second axle reaches the breakpoint of the gradient change. Hence for an estimator using powertrain inputs and potentially sensitive to large changes in demand, this behaviour will

have implications for estimator performance. Additionally, the modelling we present illustrates clearly the moments in an extreme gradient transition when further progress will be most hindered, and provides a basis for potentially improving vehicle capability in this respect.

The authors therefore assert that a further study of the dynamics of road gradient change when viewed from a vehicle perspective is both justified and a problem of substantial future interest. This problem expands on the ideas employed in step-climbing models and would ultimately lead to the development of a continuous time, forwards dynamics model applicable to the problem of continuous rapidly changing road gradient.

References

[1] H. B. Pacejka, Tyre and Vehicle Dynamics, Oxford: Butterworh-Heinemann, 2002.

[2] R. Rajamani, Vehicle Dynamics and Control, New York: Springer, 2006.

[3] W. Milliken and D. Milliken, Race Car Vehicle Dynamics, SAE Inc., 1995.

[4] J. Wong, Theory of Ground Vehiclese, New York: John Wiley and Sons Inc., 1993.

[5] P. L. a. J. E. Manfred Ploechl, "Basics of Longitudinal and Lateral Vehicle Dynamics," in *Road and Off-Road Vehicle Systems Handbook*, Boca Raton, FL., CRC Press, Taylor and Francis, 2014, pp. 971-1022.

[6] R. Wragge-Morley, G. Herrmann and P. a. B. S. Barber, "Gradient and Mass Estimation from CAN Based Data for a Light Passenger Car," *SAE International Journal of Passenger Cars– Electronic and Electrical Systems*, no. May, 2015.

[7] R. Wragge-Morley, G. Herrmann, P. Barber and S. Burgess, "Information fusion for vehicular systems parameter estimation using an extended regressor in a finite time estimation algorithm," in *IEEE/UKACC Conference on Control 2014*, Loughborough, U.K., 2014.

[8] E. Raffone, "Road Slope and Vehicle Mass Estimation for Light Commercial Vehicle using Linear Kalman Filter and RLS with forgetting factor integrated approach," in *16th International Conference on Information Fusion*, Istanbul, Turkey, 2013.

[9] M. N. Mahyuddin, J. Na, G. Herrmann, X. Ren and P. Barber, "An Adaptive Observer-based Paramter Estimation Algorithm with Application to Road Gradient and Vehicle Mass Estiamtion," in *IEEE UKACC International Conference on Control 2012*, Cardiff, U.K., 2012.

[10] M. N. Mahyuddin, J. Na, G. Herrmann, X. Ren and P. Barber, "Adaptive Observer-based Paramter Estimation with Application to Road Gradient an Vehicle Mass Estimation," *IEEE Transactions on Mechatronics*, vol. 61 no 6, 2014.

[11] P. Sahlholm and K. H. Johansson, "Road grade estimation for look-ahead vehicle control using multiple measurement runs," *Control Engineering Practice*, vol. 18, pp. 1328-1341, 2010.

[12] P. Sahlholm and K. H. Johansson, "Segmented road grade estimation for fuel efficient heavy duty vehicles," in *IEEE Conference on Decision and Control*, Atlanta, Georgia, 2010.

[13] H. Jansson, E. Kozica, P. Sahlholm and K. H. Johansson, "Improved road grade estimation using sensor fusion," in *Reglermte Conference*, Stockholm, Sweden, 2006.

[14] A. Vahidi, M. Druzhinina, A. Stefanopoulou and H. Peng, "Simultaneous Mass and Time-Varying Grade Estimation for Heavy-Duty Vehicles," in *Proceedings of the American Control Conference*, Denver, Colorado, 2003.

[15] J. Na, G. Herrmann, X. Ren, M. N. Mahyuddin and P. Barber, "Robust Adaptive Finite-Time Parameter Estimation and Control of Nonlinear Systems," in *IEEE Multi-Conference on Systems and Control*, Denver, Colorado, 2011.

[16] M. L. McIntyre, T. J. Ghotikar, A. Vahidi, X. Song and D. M. Dawson, "A Two-Stage Lyapunov-Based Estimator for Estimation of Vehicle Mass and Road Grade," *IEEE Transactions of Vehicular Technology*, Vols. 58, no. 7, pp. 3177-3185, 2009.

[17] R. Rajamani, D. Piyabongkarn, V. Tsourapas and J. Y. Lew, "Paramter and State Estimation in Vehicle Roll Dynamics," *IEEE Transactions on Intelligent Transportation Systems*, vol. 12 no. 4, pp. 1558-1567, 2011.

[18] W. Matschinsky, "Suspension Systems," in *Road and Off-Road Vehicle Systems Handbook*, Boca Raton, FL., CRC Press, Taylor and Francis, 2014, pp. 727-768.

[19] W. J. k. E. B. Spangler, GMR Road Profilometer, a method for measuring road profile, Detroit: General Motors Research Laboratories, 1964.

[20] M. W. Sayers and T. D. G. a. C. A. V. Queiroz, The International Road Roughness Experiment, Washington, D.C.: The World Bank , 1986.

[21] Y. D. a. N. M. H. Imine, "Road profile inputs for evaluation of the loads on the wheels," *Vehicle System Dynamics*, vol. 43, pp. 359-369, 2005.

[22] M. Doumiati, A. Victoriano, A. Charara and G. B. e. al., "An estimation process for vehicle wheel-ground contact normal forces," in *The International Federation of Automatic Control 17th World Congress*, Seoul, Korea, 2008.

[23] R. E. Kalman, "A new approach to linear filtering and prediction problems," *Transactions of the ASME-Journal of Basic Engineering*, vol. 82, no. Series D., pp. 35-45, 1960.

[24] G. H. Hohl, "Off Road Vehicles (Wheeled and Tracked)," in *Road and Off-Road Vehicle System Dynamics Handbook*, Boca Raton, FL, CRC Press, Taylor and Francis, 2014, pp. 395-476.

Acknowledgments

The authors wish to acknowledge the support of Jaguar Land Rover research for their continued work in the field of vehicle parameter estimation.

Nomenclature

$\boldsymbol{C_\mu}$	Rolling resistance coefficient, sometimes written as being dependent on speed as $C_\mu(\dot{s})$
$\boldsymbol{F_{drive_f}}/\boldsymbol{F_{drive_r}}$	Driving force applied at front or rear contact patches, a function of driving torque.
$\boldsymbol{F_f}/\boldsymbol{F_r}$	Net contact patches at front and rear
$\boldsymbol{F_m}$	Net forces acting at the centre of mass
$\boldsymbol{F_{RR_f}}/\boldsymbol{F_{RR_r}}$	Rolling resistance forces at front and rear, a function of normal reaction load through the tyre.
$\boldsymbol{F_v}$	Velocity dependent drag forces acting on the vehicle body
$\boldsymbol{I_m}$	Vehicle body moment of inertia
$\boldsymbol{L_c}$	Wheelbase length
$\boldsymbol{L_f}/\boldsymbol{L_r}$	Length from centre of mass to front and rear contact patches respectively, parallel to the vehicle wheelbase
$\boldsymbol{M_f}/\boldsymbol{M_r}$	Driving torques applied at front and rear axles
$\boldsymbol{R_f}/\boldsymbol{R_r}$	Normal reaction forces at front and rear
$\boldsymbol{a_m}$	Acceleration at the centre of mass
$\boldsymbol{g}$	Gravitational constant 9.81 ms^{-2}
$\boldsymbol{s_{com}}$	Displacement of the centre of mass on its trajectory
$\boldsymbol{s_f}/\boldsymbol{s_r}$	Displacement of front and rear contact patches on their respective road segments
$\boldsymbol{s_{x_f}}/\boldsymbol{s_{x_r}}$	Horizontal displacement in space of front and rear contact patches
$\boldsymbol{s_{y_f}}/\boldsymbol{s_{y_r}}$	Vertical displacement in space of front and rear contact patches
$\boldsymbol{\alpha}$	Angular acceleration of vehicle body, ie: $\ddot{\theta}_c$
$\boldsymbol{\theta_{aoc}}$	Direction of centre of mass acceleration
$\boldsymbol{\theta_c}$	Angle of inclination of the vehicle body
$\boldsymbol{\theta_{com}}$	Direction of tangent to the centre of mass trajectory
$\boldsymbol{\theta_{R_0}}/\boldsymbol{\theta_{R_r}}$	Road angle on initial (rear) path segment
$\boldsymbol{\theta_{R_1}}/\boldsymbol{\theta_{R_f}}$	Road angle on first subsequent (front) path segment

Definitions/Abbreviations

LCPC	Laboratoire central des ponts et chaussées
NVH	Noise, Vibration and Harshness

Appendix A

Full matrix expression containing moment and force balances to be solved simultaneously:

$$\begin{bmatrix} I_m\alpha_m \\ ma_m\cos\theta_{aoc} \\ ma_m\sin\theta_{aoc}+mg \end{bmatrix} = \begin{bmatrix} L_f(\cos\theta_1 - C_\mu\sin\theta_1) & L_r(-\cos\theta_6 - C_\mu\sin\theta_6) & \frac{1}{r}(L_f\sin\theta_1 + L_r\sin\theta_6)+2 \\ -\sin\theta_{R_f} - C_\mu\cos\theta_{R_f} & -\sin\theta_{R_r} - C_\mu\cos\theta_{R_r} & \frac{1}{r}(\cos\theta_{R_f} + \cos\theta_{R_r}) \\ \cos\theta_{R_f} - C_\mu\sin\theta_{R_f} & \cos\theta_{R_r} - C_\mu\sin\theta_{R_r} & \frac{1}{r}(\sin\theta_1 + \sin\theta_6) \end{bmatrix} \begin{bmatrix} R_f \\ R_r \\ M \end{bmatrix}$$